Flexible and Printed Electronics

PAPER

Metal-phthalocyanine modified doped polyaniline for VOC sensing applications

RECEIVED
9 September 2019

REVISED
19 November 2019

ACCEPTED FOR PUBLICATION
5 February 2020

PUBLISHED
2 March 2020

Mousumi Sinha[1,2,3], **Prabha Verma**[1,2,3] **and Siddhartha Panda**[1,2]

[1] Department of Chemical Engineering, Indian Institute of Technology Kanpur, Kanpur 208016, India
[2] National Centre for Flexible Electronics, Indian Institute of Technology Kanpur, Kanpur 208016, India
[3] Authors have equally contributed.

E-mail: spanda@iitk.ac.in

Keywords: phthalocyanine, polyaniline structures, sensor array, principal component analysis

Abstract

The identification and measurement of volatile organic compounds (VOCs) is needed in a variety of applications including air quality monitoring, air pollution measurement, food quality monitoring, and breath analysis-based disease diagnosis etc. The monitoring of the VOCs related to different applications areas can ensure quality health and safety. Arrays of chemical sensors have the features to provide the required identification and measurement of the VOCs. Chemical sensors made from nanostructures of polyaniline (PANI) as the base sensing material have several advantages including tunable properties, room temperature sensing and the potential of being amenable to the printing processes. Metal (M) phthalocyanines (Pc), on account of different cavity structures, have the ability to selectively interact with different gases. In the reported studies most of the MPcs have been non-covalently deposited on the sensing platforms, or attached with the base polymer via π-π conjugation. The covalent bonding of MPcs with the sensing polymer may have several possible advantages including stability (no leaching or evaporation of the compounds), well-defined available interfaces for interaction and a longer operational lifetime. In this work, the camphor sulphonic acid (CSA) doped PANI nanostructures were covalently bonded with six metal embedded phthalocyanines (Cu-Pc, Mn-Pc, Zn-Pc, Fe-Pc, Ni-Pc and Co-Pc) and investigated as the sensor materials for the sensing of four VOCs: acetone, isopropanol, ethanol and formaldehyde, in a 150–500 ppb concentration range. The resultant chemical sensor array response in terms of relative change in resistance of the sensing materials upon VOC exposure was analysed using principal component analysis, which resulted in clear discrimination among the subjected VOCs, thus making it useful for selective VOC sensing applications.

1. Introduction

The identification and measurement of volatile organic compounds (VOCs) is important in a variety of areas including the detection and monitoring of hazardous gases causing environmental pollution, food quality monitoring, indoor air quality monitoring and breath analysis for medical diagnosis [1, 2]. Chemical sensor array-based sensing systems possess the advantages of real-time detection of VOCs, low cost of material processing, miniaturization of the sensor structure with portability [3–6]. Nano-engineered materials comprising nanostructures (e.g. nanobelts, nanowires, nanotubes and nanoribbons) have shown potential for the development of chemical sensors because of enhanced adsorption capacity due to higher surface area to volume ratio, and possible modulation of physiochemical properties like electrical resistance, capacitance etc [7, 8]. Polyaniline (PANI) having advantages of the ease of synthesis, tunable properties and low cost of fabrication [9–11], offers enhanced sensitivity, fast response, room temperature sensing [12–14] and are amenable to print processesing. Recently, camphor sulfonic acid (CSA)-doped PANI structures have been used for the sensing of acetone, toluene, methanol, ethanol, isopropanol and formaldehyde [15, 16].

Monitoring of VOCs in the indoor air and controlling them to a permissible safe limit is a health issue with evidence of Sick Building Syndrome [1]. Indoor

air pollutants [17] especially VOCs such as acetone [18], formaldehyde [19], isopropanol [20], and ethanol [21, 22] come from paint, cleaning sprays, and different household utilities. In the field of food quality monitoring [23], freshness of fruits, vegetables as well as packaged food has been correlated with the VOC emission from the food, where precise VOC measurement can help in quality assessment and control of food items [24]. The composition of exhaled breath contains important information about the health of the person as certain VOCs have been indicated as disease biomarkers [2, 25–28]. Among them, acetone has been indicated as a biomarker for diabetes [28], lung cancer [29, 30], and chronic liver disease [31]; ethanol has been considered as one of the biomarkers for diabetes [28]; isopropanol [29, 30, 32] and formaldehyde [33] were reported as biomarkers of lung cancer in different studies. Therefore, the selective detection of such VOCs may help in indoor air quality monitoring, industrial pollution measurement, food quality monitoring, and breath analysis-based disease diagnosis.

Selective sensing of the VOCs is an important performance parameter of a chemical sensor array. Phthalocyanines (Pcs) embedded with different metals provide cavities with specific dimensions which promote selective binding of different chemical species resulting in selective sensing [34–37]. Most of the Pcs used for chemical sensing have been deposited on platforms with non-covalent binding such as vacuum deposited films of H_2Pc, PbPc [34], CuPc [35, 36] for NO_2 sensing, self-assembled film of Cu(II) 1,4,8,11,15, 18,22,25-octabutoxy-29H,31H-phthalocyanine nanowires for Cl_2 sensing [37], vacuum deposited films of metallophthalocyanines (CoPc, NiPc, CuPc, ZnPc and H_2Pc) for sensing vapor phase electron donors such as dichloromethane, acetonitrile, nitromethane etc [38]. In conjugated polymers, phthalocyanines have been incorporated by non-covalent binding [39]; specifically with PANI, there are reports of non-covalent attachment of different metallophthalocyanines such as tetra-β-carboxyphthalocyanine cobalt(II) mediated PANI-carbon nanotubes [40] for NH_3 sensing, films of CuPc-PANI, polypyrrole-CuPc and polythiophene-CuPc for NO_2 sensing [41], PANI/FeTsPc films for dopamine sensing [42], and PANI-chloroaluminium phthalocyanine film for CO_2 sensing [43]. While there are reports of π-π conjugation [40, 41], we are not aware of any report on having covalent attachment of MPcs with PANI for sensing of VOCs. This is the motivation of the present work. Covalent attachment of MPcs with PANI offers the possibility of better stability of the sensor surface during utilization [44] and well-defined interfaces for analyte interaction [45], along with the combined advantages of MPcs and PANI [46].

In this study, CSA-doped PANI structures were covalently functionalized with six different metal embedded Pcs utilizing the chemical interfacial polymerization route. The chemical composition and bonding involved in functionalized PANI structures were characterized by Fourier transform infrared spectroscopy (FTIR) and x-ray photoelectron spectroscopy (XPS) analysis. Morphology of the sensor material was observed with the help of field emission scanning electron microscopy (FESEM) and transmission electron microscopy (TEM) analysis. A sensor array is defined here as a collection of a number of sensors. In this work, a sensor array based on the six PANI-MPcs sensing elements was constituted and exposed to four VOCs such as acetone, ethanol, isopropanol and formaldehyde in N_2 environment. The VOC discrimination ability of a sensor array can be analyzed by using various pattern recognition techniques like principal component analysis (PCA), cluster analysis, artificial neural network, fuzzy methods etc [47, 48]. In this work PCA was utilized for analyzing the data for the detection and identification of the subjected VOCs. PANI functionalized with a combination of MPcs showed discriminatory identification of the subjected VOCs and thus could be used in a sensor array for selective VOC sensing applications.

2. Experimental

2.1. Material preparation

Doped PANI structures functionalized with different metal embedded Pcs were prepared by interfacial chemical oxidative polymerization of aniline (Sigma Aldrich, $\geqslant$99.5% pure assay) using ammonium persulfate (APS) (Sigma Aldrich, 98% pure assay) as the oxidant and camphor sulfonic acid (CSA) (Sigma Aldrich, 99% pure assay) as the dopant. The organic phase was prepared containing 5 mmol of aniline in 100 ml hexane, while the aqueous phase was prepared by dissolving 10 mmol of APS in 200 ml DI water along with 2.5 mmol of CSA and 0.1 mmol of MPc. Six different types of metal embedded phthalocyanines used were copper (II) (Sigma Aldrich, dye content >99.0%), manganese (II) (Sigma Aldrich, dye content >85.0%), zinc (Sigma Aldrich, dye content >97.0%), iron phthalocyanines (Sigma Aldrich, dye content >90.0%), nickel (II) (Sigma Aldrich, dye content >85.0%) and cobalt (II) (Sigma Aldrich, β form, dye content >97.0%). All chemicals were used as received without any further purification before experimentation. Then the aqueous phase was mixed gradually into the organic phase and two separate phases were generated. The resulting mixture was kept undisturbed for 12 h at 5 °C. Then the material was filtered, sequentially washed with DI water, as well as acetone followed by vacuum drying at 60 °C for 48 h. In this study, the CSA-doped PANI structures functionalized with the six metal embedded Pcs are termed as PANI-CuPc, PANI-MnPc, PANI-ZnPc, PANI-FePc, PANI-NiPc and PANI-CoPc.

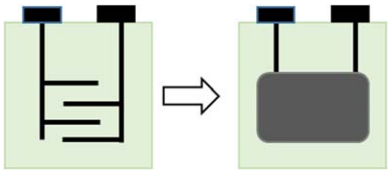

Figure 1. Schematic of the interdigitated electrodes and the drop casted sensing material.

2.2. Material characterization

FTIR spectra of doped PANI functionalized with metal Pcs were obtained from a spectroscope (BrukerTM Vertex-70) on KBr pellets for a range of 4000–400 cm^{-1} with a resolution of 8 cm^{-1}. X-ray photoelectron spectra were obtained for films mounted onto sample stubs utilizing a scanning XPS microprobe (PHI5000 versaprobe II, ULVac-PHI, Inc.) with a monocromated AlKα x-ray gun. Pass energies of 187.85 eV and 23.5 eV were utilized for the survey spectra and elemental core-line spectra respectively. The atomic percentage composition was quantified from the high resolution spectra with the sensitivity factors provided by the manufacturer. Spectra alignment was done to the hydrocarbon component with C1s peak set at 285 eV. Transmission electron microscopy (FEI-Titan XFEG G2) and field emission scanning electron microscopy (Tescan MIRA3) was utilized for morphology studies. The TEM samples were prepared by drop-casting 6 μl dispersed MPcs in DI water over 300 mesh carbon coated Cu grid.

2.3. Fabrication of the sensing element

Interdigitated copper electrodes were printed on a transparent 180 μm thick flexible PI substrate with bands/gap dimension of 400 μm. In a typical preparation method, 0.05 gm of the structured powder was mixed with 500 μl of DI water in a sample vial. Then the mixture was drop casted on a copper interdigitated circuit (5 mm × 5 mm) using the Doctor's blade method and kept in a vacuum oven for drying at 60 °C for 4 h. The typical size of the drop casted film was kept fixed at 0.5 cm × 0.4 cm × 0.1 cm. The schematic of the copper interdigitated circuit board and the drop casted sensor are shown in figure 1.

2.4. Design and fabrication of the sensor system

An in-house VOC sensing setup was fabricated and used in this study. Figure 2 shows the schematic view of the sensing system. It consisted of a VOC vapor generator, a mixing chamber for the mixing of the vapor with the N_2 for achieving the desired analyte concentration, a sensing chamber for the sensing of VOCs through the sensor films, and a data acquisition system for acquisition of the sensor array response. N_2 was used as the carrier gas. After every successful sensing study, inert gas was purged for flushing out the residual vapors from the sensing chamber. The N_2 gas line flow is divided into two parts, where one goes to the vapor generator section and other goes directly to the sensing chamber through the mixing chamber. N_2 flow was controlled separately in these two lines with the help of a mass flow controller and separate high precision needle valves. First, the inert environment was created in the sensing chamber by flowing only N_2 through it, to avoid any degradation of the sensing surface from moisture. Then, a controlled amount of N_2 was flowed into the vapor generator section, which consists of a bubbler with a particular amount of analyte (VOC), the analyte vapor was carried to the mixing chamber, where the analyte vapors were mixed with N_2 in a particular proportion to achieve the desired VOC concentration, and then fed to sensing chamber and exposed to the sensor film for 600 s. An additional exhaust was used for system safety for avoiding unwanted pressure build-up in the flow lines. A similar kind of setup was utilized in several works [49, 50] and thus is considered here. The calibration of the VOC concentrations generated from the developed setup was performed utilizing a set of commercial metal oxide sensors. The sensor response was measured as the relative change in resistance of the sensor film due to VOC exposure. All the measurements were conducted at a relative humidity (R_H) of 25% and a temperature range between 20–25 °C. After adsorption, residual vapors were flushed out of the system utilizing N_2 flow. All the measurements were conducted in triplicate and the error bars indicated one standard deviation.

2.5. Electrical characterization

I–V measurements for VOC responses were conducted in the range of 0–4 V by an I–V measurement system (Keithley 2602A). Considering R_0 as pristine resistance of the sensor material and R is the resistance of the sensor material after exposure to the analyte vapor, the response of VOC sensor (R_s) is defined as the ratio of the change in resistance of the sensor due to exposure to analyte vapor to the pristine resistance of the sensor as shown in equation (1).

$$R_s(\%) = \frac{(R - R_0) \times 100}{R_0}. \quad (1)$$

3. Results and discussion

3.1. Material characterization and morphology characterization

FTIR spectrographs of the six PANI-MPcs structures are shown in figures 3(a)–(f). The spectra are similar, and the peak positions corresponding to the oxidation of the polymer, different bond stretchings, and ring positions etc match well with the available literature values of doped PANI [41]. Particularly, peaks obtained around 3433 cm^{-1}, 2920 cm^{-1}, 1570 cm^{-1}, 1488 cm^{-1}, 1300 cm^{-1}, 505 cm^{-1} and 1170 cm^{-1} correspond to

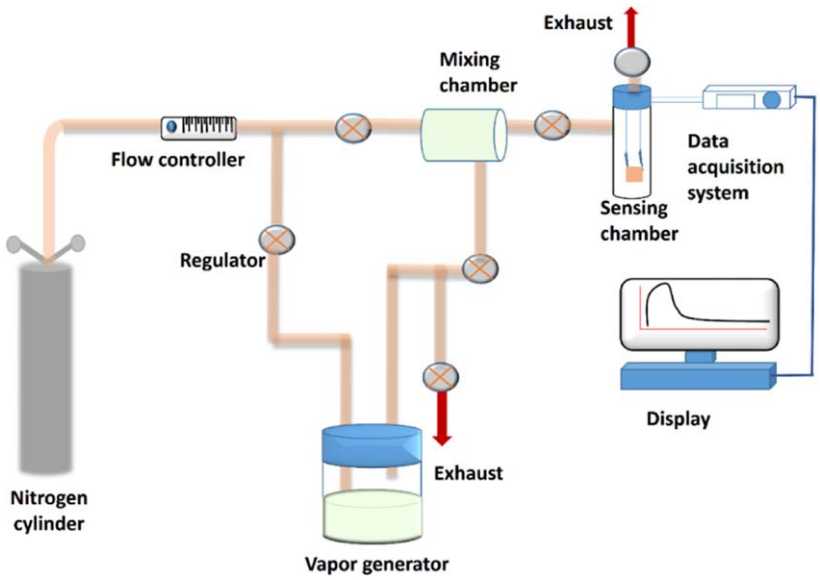

Figure 2. VOC sensing and measurement setup.

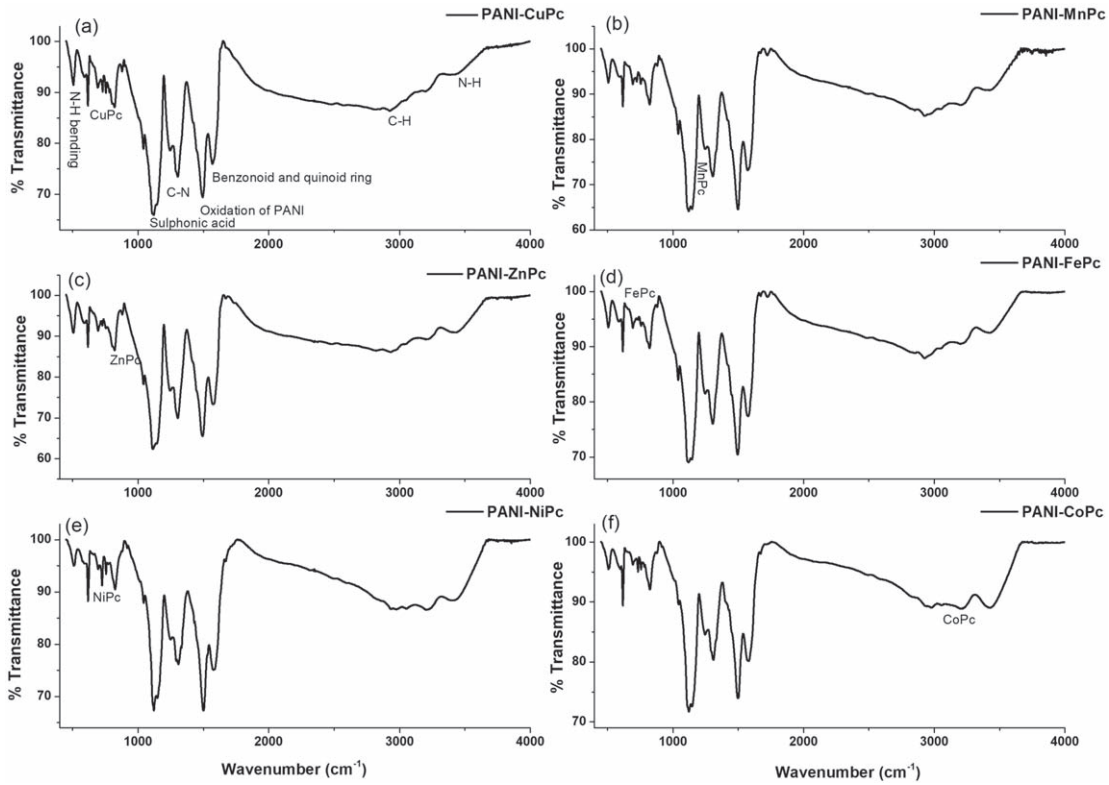

Figure 3. FTIR spectrographs of doped PANI functionalized with (a) CuPc, (b) MnPc, (c) ZnPc, (d) FePc, (e) NiPc and (f) CoPc.

N–H bond stretching, C–H bond stretching, the quinoid and the benzenoid ring in the polymer, oxidation of the polymer, C–N bond stretching, N–H out-of-plane bending and presence of the sulphonic acid group in the polymer as the dopant, respectively [41]. The presence of different MPcs was also confirmed from literature. Peaks around 730 cm^{-1}, 754 cm^{-1}, 772 cm^{-1} and 780 cm^{-1} confirmed the presence of CuPc in the PANI-CuPc complex [41]; peaks around 1598 cm^{-1}, 1124 cm^{-1}, 1018 $cm^{-1}$and 756 cm^{-1} confirmed the presence of MnPc in the PANI-MnPc complex [51]; peaks around 721 cm^{-1}, 3100 cm^{-1}, 1652 cm^{-1}, 1498 cm^{-1} confirmed the presence of CoPc in the PANI-CoPc complex [51]. Peaks around 730 cm^{-1}, 755 cm^{-1} and 779 cm^{-1} confirmed the presence of NiPc in the PANI-NiPc complex [42]; peaks around 729 cm^{-1} and 750 cm^{-1} confirmed the presence of FePc in the PANI-FePc complex [42]; and

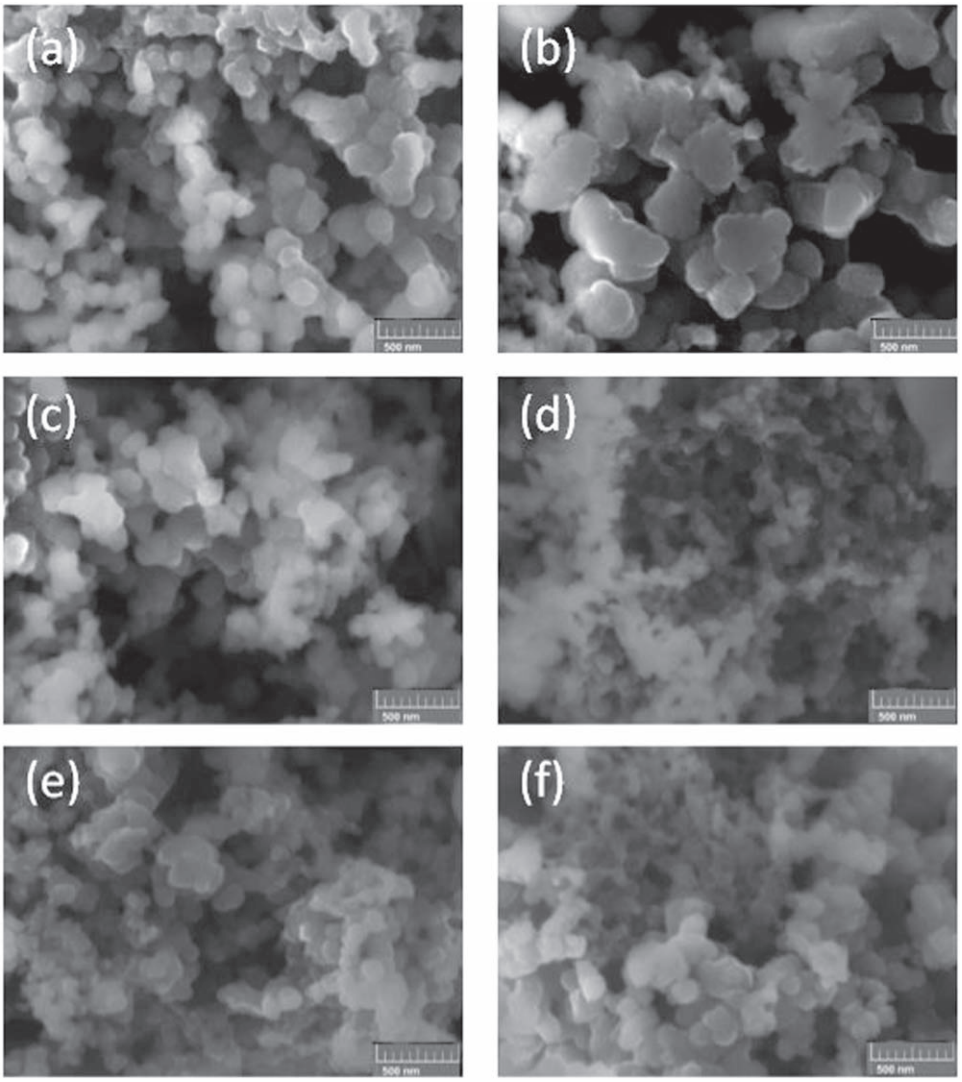

Figure 4. Scanning electron micrographs of the PANI structures functionalized with (a) CuPc, (b) MnPc, (c) ZnPc, (d) FePc, (e) NiPc and (f) CoPc.

peaks around 700 cm^{-1} and 800 cm^{-1} confirmed the presence of ZnPc in the PANI-ZnPc complex [51].

Morphologies of the six different types of MPcs were studied by FESEM, which are shown in figures 4(a)–(f). Although the initial composition of doped PANI was same for six types of complexes, but the variation in morphology was observed because of different nature of the MPcs. Globular structures of sizes 35–100 nm were seen for PANI-CuPc, while those of sizes 50–250 nm was seen for PANI- MnPc. Agglomerates in the size range 50–150 nm was seen for PANI- ZnPc. PANI-FePc was fibrous in nature with characteristic sizes less than 50 nm. PANI-NiPc and PANI-CoPc displayed a mixture of fibrous and globular morphologies with sizes 50–250 nm.

Micrographs from TEM study for sensor materials showed consistent results with that of the SEM study and are shown in figures 5(a)–(d) for PANI structures functionalized with (a) CuPc, (b) MnPc, (c) ZnPc, (d) CoPc respectively. Micrographs for PANI-FePc and PANI-NiPc were not possible due to magnetic issues during imaging. Globular structures of sizes 40–100 nm for PANI- CuPc and sizes of 50–200 nm for PANI-MnPc were observed. Agglomerates in the size range 50–150 nm were observed for PANI- ZnPc. Mixed morphologies consisting of fibrous and globular structures were observed for PANI- CoPc with sizes 50–250 nm.

Compositional analysis was carried out utilizing XPS to investigate the nature of attachment of MPcs with the doped PANI. XPS survey spectra, atomic composition, deconvoluted spectra for N1s, O1s, S2p, C1s, and Cu2p of doped PANI functionalized with CuPc were studied and are shown in figures 6(a)–(g) respectively.

Survey spectra of PANI-CuPc confirmed the presence of Cu2p3 (for CuPc), S2p (for CSA), N1s, C1s (for PANI) and O1s (for oxidation of aniline), as shown in figure 6(a). Atomic percentage spectra (figure 6(b)) confirmed the comparative composition

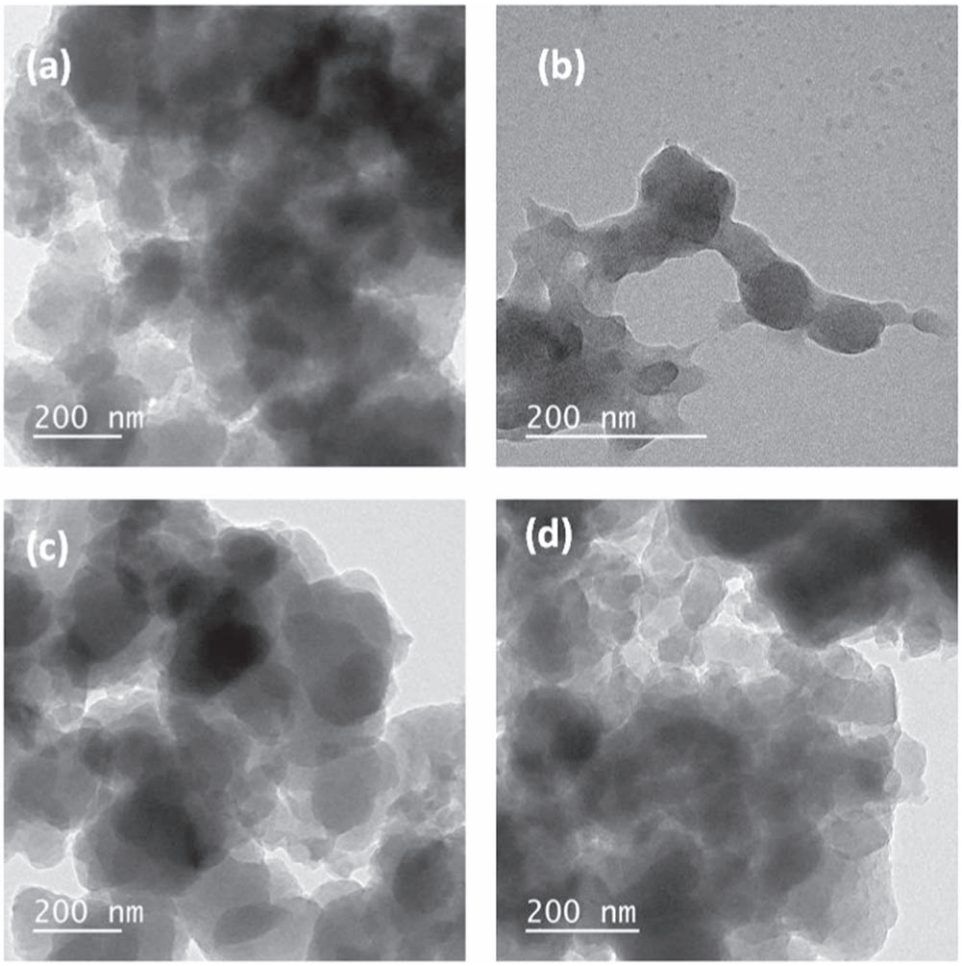

Figure 5. Transmission electron micrographs of the PANI structures functionalized with (a) CuPc, (b) MnPc, (c) ZnPc, (d) CoPc.

of the elements. From the deconvoluted spectra analysis, the presence of PANI, dopant, CuPc, and covalent bonding between CuPc and PANI—CSA in PANI-CuPc were confirmed as follows (figures 6(c)–(g)). C1s spectra shows the presence of C–C and C–O interactions. In N1s spectra, the protonated quinonoid ring presence was observed. A similar analysis was conducted for the O1s spectra where the presence of C=O and C–O bonds were observed. S2p signal corresponds to the dopant sulphonate anion affixed covalently with the main PANI chain. The spin–orbit doublet S2p1/2 and S2p3/2 confirmed dopant attachment to the main PANI backbone. Cu2p3 signal corresponds to the CuPc affixed covalently with the main PANI chain. The spin–orbit doublet Cu2p1/2 and triplet Cu2p3/2 confirmed Pc attachment to the main PANI backbone. Similar studies conducted for other PANI-CSA-MPcs (not shown here) confirmed the covalent bonding of MPcs with PANI.

3.2. VOC sensing studies

The fabricated sensor films labeled as PANI-CuPc, PANI-FePc, PANI-MnPc, PANI-NiPc, PANI-ZnPc, PANI-CoPc were studied for VOC sensing. VOC sensing studies were conducted with different concentrations of ethanol, isopropanol, acetone and formaldehyde in N_2 atmosphere. Screening experiments were conducted to choose the values of the concentrations to be studied, and based on these, for all analytes 150, 250, and 500 ppb were used. The percentage responses of PANI-CuPc to 150 ppb of ethanol, isopropanol, acetone and formaldehyde as a function of time are shown in figure 7(a). Resistance of the sensor materials increased with exposure to ethanol and isopropanol, whereas for acetone and formaldehyde, the resistance decreased. Response time was calculated as the time taken by the sensor to reach 63.3% of the maximum response with the exposure of analytes. As seen from figure 7(a), response time with exposure to 150 ppb of all analytes of PANI-CuPc were about 2.5 min for ethanol, 2 min for isopropanol, 4 min for formaldehyde and 3.5 min for acetone, respectively. The percentage response values at the saturated condition were about 32.0 for ethanol, 14.0 for isopropanol, 6.0 for formaldehyde and 1.2 for acetone, respectively. Comparative saturated percentage response of all of the studied PANI-MPcs (PANI-CuPc, PANI-FePc, PANI-MnPc, PANI-NiPc, PANI-ZnPc, PANI-CoPc) to 150 ppb of four VOCs (ethanol,

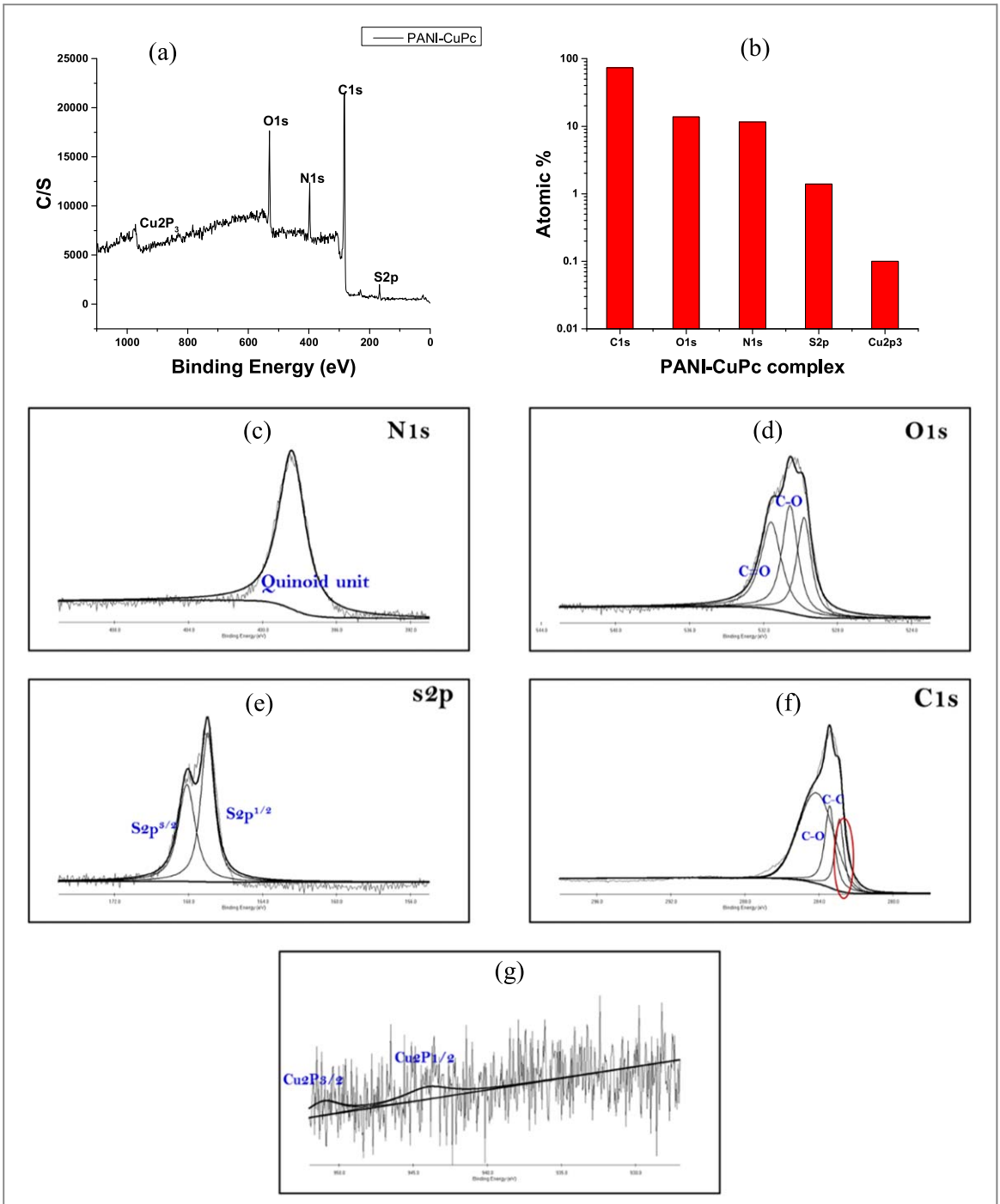

Figure 6. XPS spectroscopy of PANI structures functionalized with CuPc (a) XPS survey spectra, (b) atomic composition, deconvoluted spectra for (c) N1s, (d) O1s, (e) S2p, (f) C1s, and (g) Cu2p respectively.

isopropanol, acetone and formaldehyde) were studied and shown in figure 7(b). With acetone exposure, a decrease in resistance was seen for all the complex material studied here, whereas for all other three analytes, a different kind of response characteristics was seen. Also for a similar nature of response characteristics (increase or decrease), response time was varied with different kinds of VOC. Collective responses of the sensor elements were analyzed as the sensor array for the VOC sensing application.

The saturated response value from all the sensors corresponding to the VOCs is presented in table 1. These response values are used for analyzing the VOC discrimination ability of the sensor array using principal component analysis.

Sensitivity studies were done for all the PANI-MPcs to the studied analytes (ethanol, isopropanol, acetone and formaldehyde). Sensitivities were calculated from the characteristic curve of response versus analyte concentration. Calibration plots for all six types of complexes for isopropanol, formaldehyde, ethanol and acetone is shown in figures 8(a)–(d). Sensitivity was calculated from the slope of response versus concentration plots. For all the analytes studied

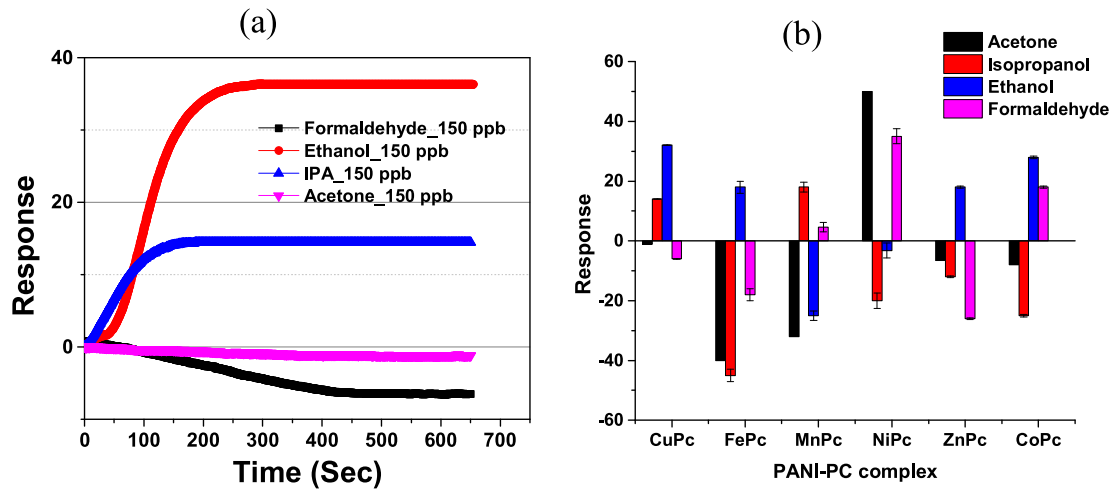

Figure 7. Responses of doped PANI structures functionalized with MPc to VOCs (a) characteristic curve of PANI-Cupc with the four analytes, (b) saturated response of all complexes at 150 ppb of the analytes (ethanol, isopropanol, acetone, and formaldehyde).

Table 1. Sensor array response matrix.

	CSA-doped PANI –phthalocyanine modified conducting polymer sensors						
VOCs	CuPc	FePc	MnPc	NiPc	ZnPc	CoPc	Conc. (ppb)
Acetone	−1.20	−40.01	−32.00	50.00	−6.50	−8.00	150
	−1.92	−64.00	−51.20	80.01	−10.40	−12.80	250
	−4.42	−147.20	−117.76	184.01	−23.92	−29.44	500
Isopropanol	14.00	−45.00	18.00	−20.00	−12.00	−25.00	150
	19.04	−61.20	24.48	−27.20	−16.32	−34.00	250
	34.27	−110.16	44.06	−48.96	−29.37	−61.20	500
Ethanol	32.01	18.00	−25.00	−3.20	18.00	28.00	150
	52.16	29.34	−40.75	−5.22	29.34	45.64	250
	93.88	52.81	−73.35	−9.39	52.81	82.15	500
Formaldehyde	−6.00	−18.00	4.60	35.00	−260	18.00	150
	−7.20	−21.60	5.52	42.00	−31.20	21.60	250
	−12.96	−38.88	9.936	75.60	−56.16	38.88	500

here, both positive and negative change in response was observed. Detailed bar plots for sensitivity are shown in figures 9(a)–(d). Maximum sensitivities for acetone with PANI-NiPc, formaldehyde with PANI-FePc, isopropanol with PANI-MnPc, and ethanol with PANI-CuPc, were observed.

Cross-sensitivities were observed for PANI functionalized with MPcs for some of the VOCs among the analytes studied here. Cross-sensitivities of PANI-CuPc were observed for ethanol and isopropanol. For PANI-FePc, cross-sensitivities were observed for acetone, isopropanol, and formaldehyde. Similarly, cross-sensitivities with acetone and ethanol for PANI-MnPc, acetone and formaldehyde for PANI-NiPc, acetone, isopropanol and formaldehyde for PANI-ZnPc, and ethanol and formaldehyde for PANI-CoPc were observed. Stability studies of the sensor materials were performed up to six months utilizing fresh sensor films fabricated from PANI-MPcs powder securely stored in the vacuum desiccator. One such stability plot for CuPc with the studied VOCs, each at a concentration of 500 ppb, is shown in figure 10. Stability studies indicate that the material has aging effect, although their responses could be considered to be within acceptable limits with the studied VOCS.

Sensing mechanisms of the PANI-MPcs having covalently bonded MPcs responsible for selective sensing can be explained by interaction energy of the sensing material to that of the analytes. Lower the energy barrier between them better is the interaction and the nature of the difference in their Fermi level determines the nature of interaction. In a previous work from our group, CSA-doped PANI was utilized for sensing a set of different gases such as NO_2, NH_3, CO_2, N_2 and sensing mechanism was investigated. It was observed that the energy barrier of interaction between PANI with the gases plays a key role for selective sensing [52]. Another study investigating the sensing mechanism was performed by our group considering these six kinds of MPcs (M = Cu, Mg, Mn, Co, Ni, and Zn) to several VOCs such as isoprene, acetone, ammonia, methanol, and methane utilizing DFT study with

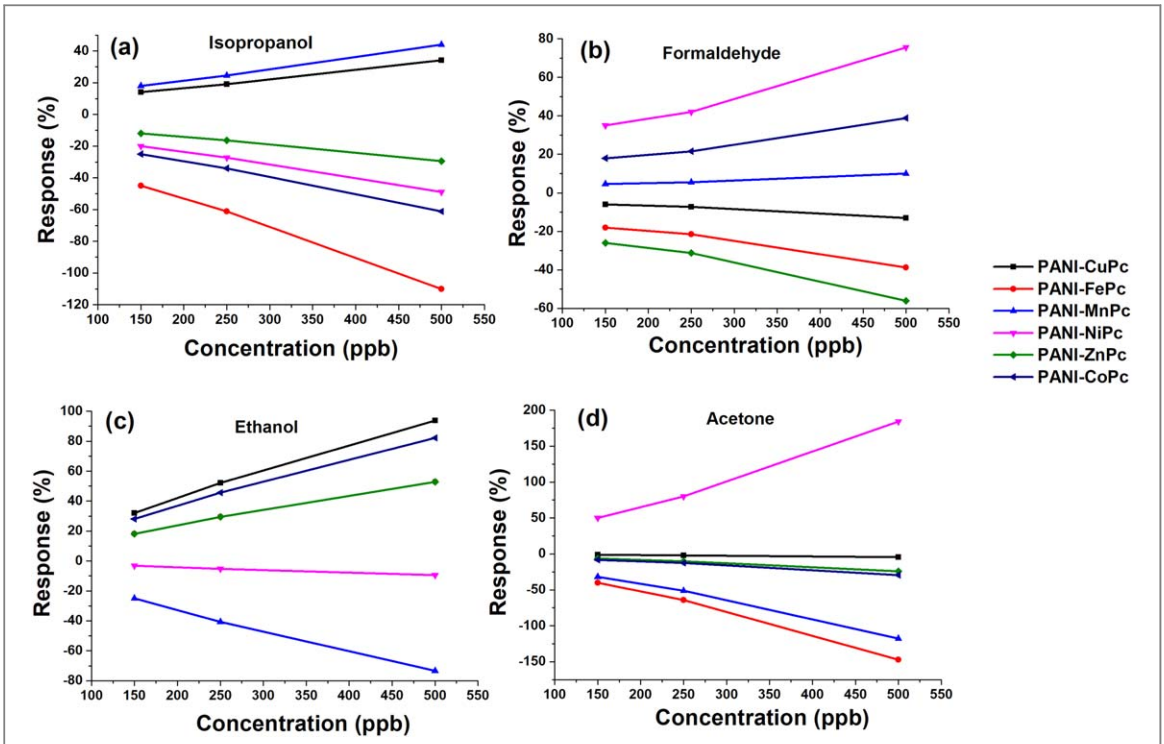

Figure 8. Sensitivities of doped PANI structures functionalized with MPcs for VOCs (a) isopropanol, (b) formaldehyde, (c) ethanol and (d) acetone.

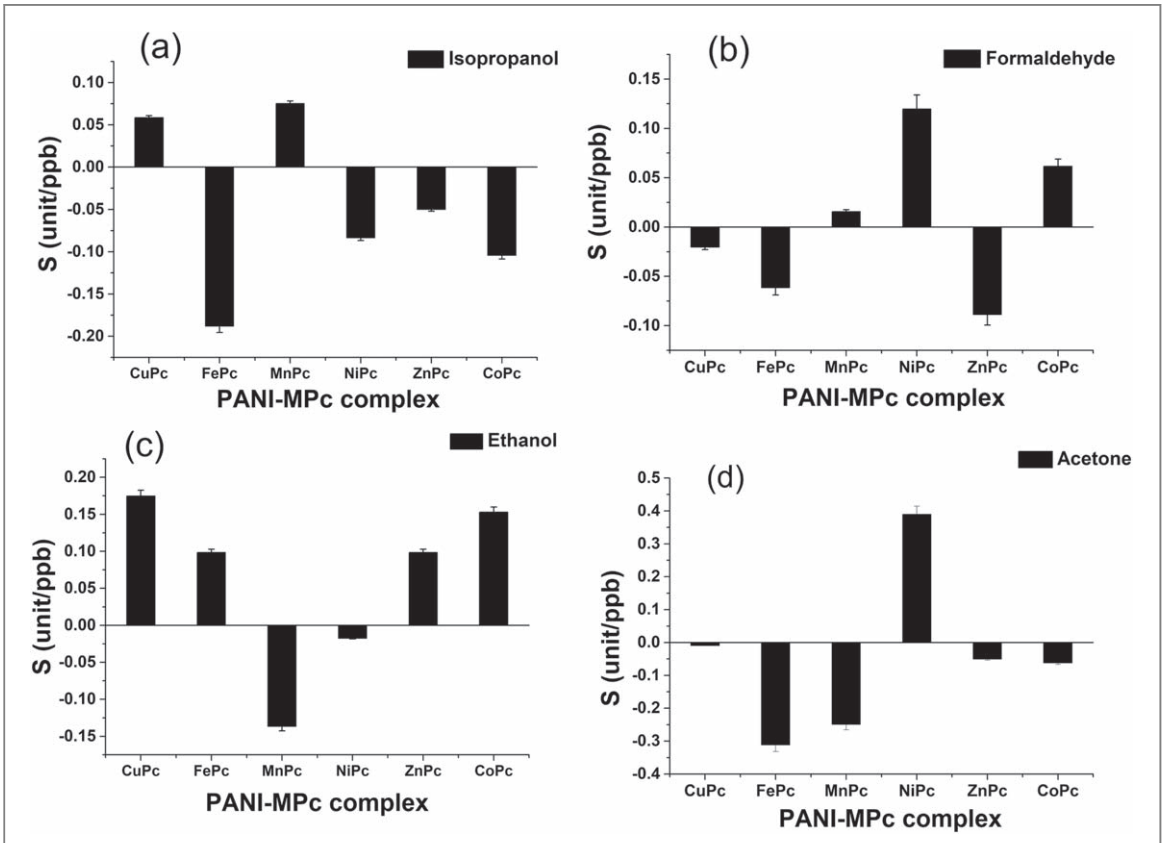

Figure 9. Compared sensitivities of doped PANI structures functionalized with MPcs in bar plot for VOCs (a) isopropanol, (b) formaldehyde, (c) ethanol, and (d) acetone.

support of experimental observations. The study attributed the selective sensing of the MPcs to their specific cavity structures and this was explained by interaction energy and energy barrier of interaction between Fermi level of the sensor material with that of the VOC molecules [53]. Detailed theoretical studies

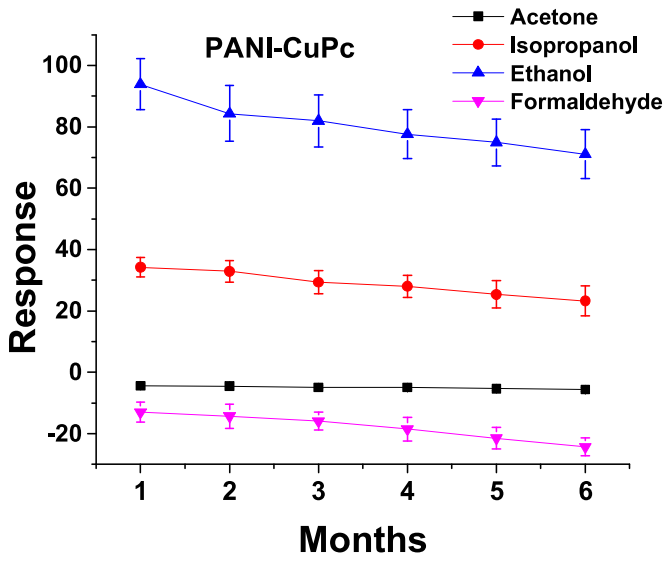

Figure 10. Responses at 500 ppb of VOCs as a function of time indicating the stability of doped PANI–CuPc.

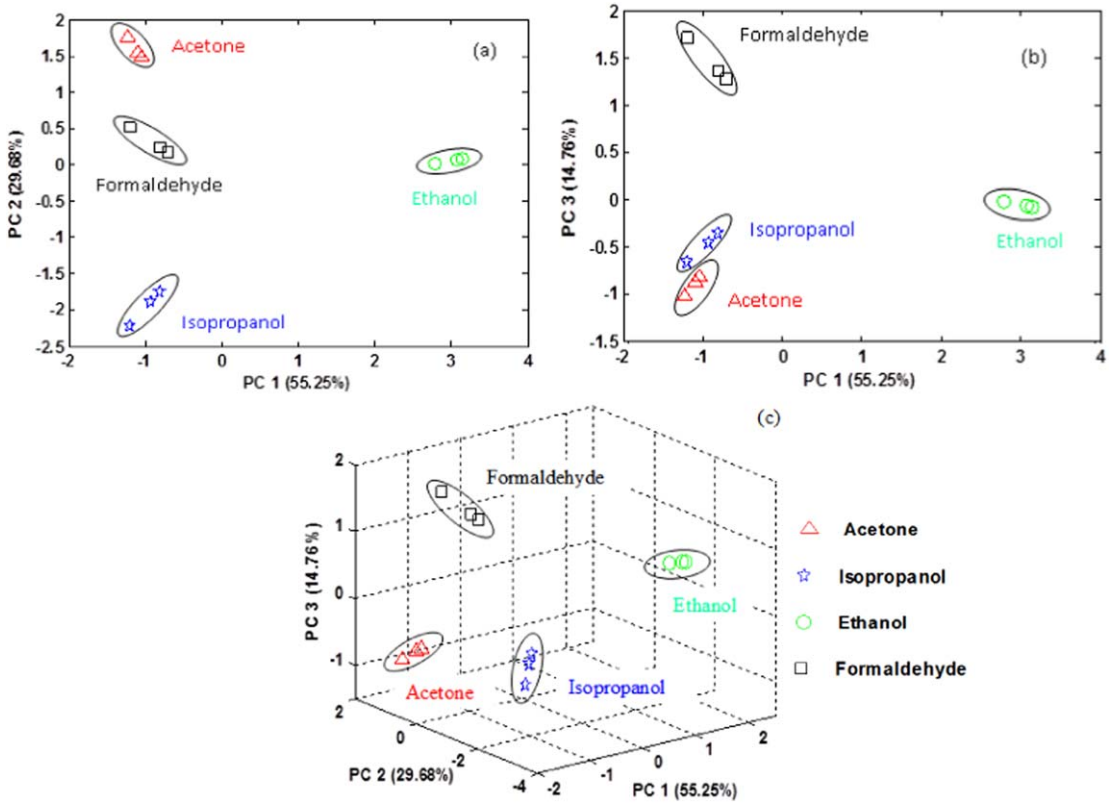

Figure 11. Principal component space plot for a six-element sensor array (a) PC1 and PC2 (b) PC1 and PC3 (c) PC1, PC2 and PC3.

of sensing mechanisms of CSA-doped PANI covalently attached with MPcs for VOC sensing is a subject of a future work.

3.3. VOC analyte recognition through PCA

Principal component analysis [47, 48] was implemented on the preprocessed sensor array response matrix, shown in table 1 for recognizing the tested VOCs. Figure 11 shows the principal component space plots for the first three principal components.

The percentage information content possessed by the principal components are also shown in figure 11. The different VOCs are represented by the different colors and symbols. In figure 11(a), the PC1 versus PC2 plot shows that ethanol, isopropanol, acetone and formaldehyde are well separated from each other and the same type of VOC samples are clustered at a place

(enclosed by an oval). Similarly, in figure 11(b) PC1 and PC3 plot, a similar trend is seen though acetone and isopropanol appear to be in proximity but nevertheless well discriminated from each other. The 3D plot in figure 11(c) contains the first three principal component directions shows that all the VOCs are well separated and discriminated in principal component space. Hence, principal component analysis established that the sensor array constituted by the fabricated PANI-MPcs structures is well suited for the detection and identification of the subjected VOCs. Knowledge generated from this work can be utilized for the functionalization of different conducting polymers and utilization as a sensor array for selective sensing of analytes.

4. Conclusions

CSA-doped PANI structures covalently bonded with six kinds of metal phthalocyanines (Cu-Pc, Mn-Pc, Zn-Pc, Fe-Pc, Ni-Pc and Co-Pc) were successfully synthesized and fabricated. From XPS spectroscopy, covalent bonding between metal Pcs with CSA doped PANI was confirmed. Four different types of VOCs – acetone, isopropanol, ethanol, and formaldehyde were used for sensing in the concentration range of ppb. Different sensor materials showed distinctive signatures upon exposure to the VOCs. PCA analysis confirmed that the fabricated PANI-CSA-Pcs sensor array could detect, identify and discriminate among the subjected VOCs and thus could be used for selective VOC sensing applications.

Acknowledgments

Funding from the Ministry of Electronics and Information Technology, grant number 2(4)/2014-PEGD (IPIIW), Government of India, is acknowledged. Prabha Verma gratefully acknowledges the financial support of DST- SERB, Govt of India (N-PDF reference no. PDF/2016/000512), for carrying out this research work.

ORCID iDs

Siddhartha Panda https://orcid.org/0000-0001-9131-4264

References

[1] Lee D-D and Lee D-S 2001 Environmental gas sensors *IEEE Sensors* **1** 214–24
[2] Konvalina G and Haick H 2013 Sensors for breath testing: from nanomaterials to comprehensive disease detection *Acc. Chem. Res.* **47** 66–76
[3] Janata J, Josowicz M and DeVaney D M 1994 Chemical sensors *Anal. Chem.* **66** 207–28
[4] Janata J 2009 *Principles of Chemical Sensors* (New York: Springer) 1–340
[5] Claramunt S, Monereo O, Boix M, Leghrib R, Prades J D, Cornet A, Merino P, Merino C and Cirera A 2013 Flexible gas sensor array with an embedded heater based on metal decorated carbon nanofibres *Sens. Actuators* B **187** 401–6
[6] Hu Y, Lee H, Kim S and Yun M 2013 A highly selective chemical sensor array based on nanowire/nanostructure for gas identification *Sens. Actuators* B **181** 424–31
[7] Castro M, Kumar B, Feller J F, Haddi Z, Amari A and Bouchikhi B 2011 Novel e-nose for the discrimination of volatile organic biomarkers with an array of carbon nanotubes (CNT) conductive polymer nanocomposites (CPC) sensors *Sens. Actuators* B **159** 213–9
[8] Hassan J J, Mahdi M A, Chin C W, Abu-Hassan H and Hassan Z 2013 A high-sensitivity room-temperature hydrogen gas sensor based on oblique and vertical ZnO nanorod arrays *Sens. Actuators* B **176** 360–7
[9] Huang W-S, Humphrey B D and MacDiarmid A G 1986 Polyaniline, a novel conducting polymer *J. Chem. Soc., Faraday Trans.* **82** 2385–400
[10] Li D, Huang J and Kaner R B 2008 Polyaniline nanofibers: a unique polymer nanostructure for versatile applications *Acc. Chem. Res.* **42** 135–45
[11] Huang J, Virji S, Weiller B H and Kaner R B 2003 Polyaniline nanofibers: facile synthesis and chemical sensors *Journal of American Chemical Society* **125** 314–5
[12] Ayad M M, Salahuddin N A, Minisy I M and Amer W A 2014 Chitosan/polyaniline nanofibers coating on the quartz crystal microbalance electrode for gas sensing *Sens. Actuators* B **202** 144–53
[13] Do J-S and Wang S-H 2013 On the sensitivity of conductimetric acetone gas sensor based on polypyrrole and polyaniline conducting polymers *Sens. Actuators* B **185** 39–46
[14] Athawale A A, Bhagwat S V and Katre P P 2006 Nanocomposite of Pd–polyaniline as a selective methanol sensor *Sens. Actuators* B **114** 263–7
[15] Bhadra S, Khastgir D, Singha N K and Lee J H 2009 Progress in preparation, processing and applications of polyaniline *Prog. Polym. Sci.* **34** 783–810
[16] Bai H and Shi G 2007 Gas sensors based on conducting polymers *Sensors* **7** 267–307
[17] Rickerby D G and Serventi A M 2010 Nanostructured Metal Oxide Gas Sensors for Air Quality Monitoring *Environanotechnology* (Amsterdam: Elsevier) pp 99–136
[18] Ying Z, Jiang Y, Qin H, Zheng L and Du X 2010 A study on QCM sensor for identification of acetone vapor *The International Journal for Computation and Mathematics in Electrical and Electronic Engineering* **29** 477–83
[19] Yusof H H M, Jali M H, Johari M A M, Dimyati K, Harun S W, Khasanah M and Yasin M 2019 Detection of formaldehyde vapor using glass substrate coated with zinc oxide nanorods *IEEE Photonics J.* **11** 1–12
[20] Ngo Y H, Brothers M, Martin J A, Grigsby C C, Fullerton K, Naik R R and Kim S S 2018 Chemically enhanced polymer-coated carbon nanotube electronic gas sensor for isopropyl alcohol detection *ACS Omega* **3** 6230–6
[21] Wang Y, Liu L, Meng C, Zhou Y, Gao Z, Li X, Cao X, Xu L and Zhu W 2016 A novel ethanol gas sensor based on $TiO_2/Ag_{0.35}V_2O_5$ branched nanoheterostructures *Sci. Rep.* **6** **33092** 1–10
[22] Mariani S, Strambini L M, Paghi A and Barillaro G 2018 Low-concentration ethanol vapor sensing with nanostructured porous silicon interferometers using interferogram average over wavelength reflectance spectroscopy *IEEE Sensors J.* **18** 7842–49
[23] Fleming-Jones M E and Smith R E 2003 Volatile orrganic compounds in foods: a five year study *J. Agric. Food Chem.* **51** 8120–7
[24] Phan P N, Kim K, Jeon E, Kim U, Sohn J and Pandey S 2012 Analysis of volatile organic compounds released during food decaying processes *Environ. Monit. Assess.* **184** 1683–92
[25] Poli D, Carbognani P, Corradi M, Goldoni M, Acampa O, Balbi B, Bianchi L, Rusca M and Mutti A 2005 Exhaled volatile organic compounds in patients with non-small cell lung

cancer: cross sectional and nested short-term follow-up study *Respiratory Research* **6** 1–10.
[26] Paredi P, Kharitonov S A, Leak D, Ward S, Cramer D and Barnes P J A J R C C M 2000 Exhaled ethane, a marker of lipid peroxidation, is elevated in chronic obstructive pulmonary disease *American Journal of Respiratory and Critical Care Medicine* **162** 369–73
[27] Högman M, Holmkvist T, Wegener T, Emtner M, Andersson M, Hedenström H and Meriläinen P 2002 Extended NO analysis applied to patients with COPD, allergic asthma and allergic rhinitis *Respiratory Medicine* **96** 24–30
[28] Galassetti P R, Novak B, Nemet D, Rose-Gottron C, Cooper D M, Meinardi S, Newcomb R, Zaldivar F and Blake D R 2005 Breath ethanol and acetone as indicators of serum glucose levels: an initial report *Diabetes Technology & Therapeutics* **7** 115–23
[29] Kischkel S, Miekisch W, Sawacki A, Straker E M, Trefz P, Amann A and Schubert J K 2010 Breath biomarkers for lung cancer detection and assessment of smoking related effects—confounding variables, influence of normalization and statistical algorithms *Clin. Chim. Acta* **411** 1637–44
[30] Wehinger A, Schmid A, Mechtcheriakov S, Ledochowski M, Grabmer C, Gastl G A and Amann A 2007 Lung cancer detection by proton transfer reaction mass-spectrometric analysis of human breath gas *Int. J. Mass spectrom.* **265** 49–59
[31] Van den Velde S, Nevens F, Van hee P, van Steenberghe D and Quirynen M 2008 GC-MS analysis of breath odor compounds in liver patients *The Journal of Chromatography* B **875** 344–8
[32] Buszewski B, Kesy M, Ligor T and Amann A 2007 Human exhaled air analytics: biomarkers of diseases *Biomed. Chromatogr.* **21** 553–66
[33] Fuchs P, Loeseken C, Schubert J K and Miekisch W 2010 Breath gas aldehydes as biomarkers of lung cancer *International Journal of Cancer* **126** 2663–70
[34] Bott B and Jones T A 1984 A highly sensitive NO_2 sensor based on electrical conductivity changes in phthalocyanine films *Sens. Actuators* **5** 43–53
[35] Dogo S, Germain J-P, Maleysson C and Pauly A 1992 Interaction of NO_2 with copper phthalocyanine thin films II' application to gas sensing *Thin Solid Films* **219** 251–6
[36] Cheng-Jun Q, Yan-Wei D, Quan-Liang Z, Wei Q, Jie Y, Yan-Mei S and Mao-Sheng C 2008 Nitrogen dioxide sensing properties and mechanism of copper phthalocyanine film *Chin. Phys. Lett.* **25** 3590–2
[37] Saini R, Mahajan A, Bedi R K, Aswal D K and Debnath A K 2014 Room temperature ppb level Cl2 detection and sensing mechanism of highly selective and sensitive phthalocyanine nanowires *Sens. Actuators* B **203** 17–24
[38] Bohrer F I, Colesniuc C N, Park J, Ruidiaz M E, Schuller I K, Kummel A C and Trogler W C 2009 Comparative gas sensing in cobalt, nickel, copper, zinc, and metal-free phthalocyanine chemiresistors *Journal of American Chemical Soceity* **131** 478–85
[39] Patois T, Sanchez J-B, Berger F, Fievet P, Segut O, Moutarlier V, Bouvet M and Lakard B 2013 Elaboration of ammonia gas sensors based on electrodeposited polypyrrole—Cobalt phthalocyaninehybrid films *Talanta* **117** 45–54
[40] Wu H, Chen Z, Zhang J, Wu F, He C, Wuab Y and Ren Z 2017 Phthalocyanine-mediated non-covalent coupling of carbon nanotubes with polyaniline for ultrafast NH3 gas sensors *J. Mater. Chem.* A **5** 24493–501
[41] Radhakrishnan S and Deshpande S D 2002 Conducting polymers functionalized with phthalocyanine as nitrogen dioxide sensors *Sensors* **2** 185–94
[42] Zucolotto V, Ferreira M, Cordeiro M A R, Constantino C J L, Moreira W A C and Oliveira O N Jr 2006 Nanoscale processing of polyaniline and phthalocyanines for sensing applications *Sens. Actuators* B **113** 809–15
[43] Azim-Araghi M E and Jafari M J 2010 Electrical and gas sensing properties of polyaniline chloroaluminium phthalocyanine composite thin films *Eur. Phys. J. Appl. Phys.* **52** 10402 -p1-p6
[44] Tao J 2012 Covalent attachment of functionalized polyaniline nanofibers onto graphene oxide *Journal of Material Research Society* **27** 2644–9
[45] Zeng R, Li Z, Li L, Li Y, Huang J, Xiao Y, Yuan K and Chen Y 2019 Covalent connection of polyaniline with MoS_2 nanosheets toward ultrahigh rate capability supercapacitors *ACS Sustainable Chemical Engineering* **7** 11540–9
[46] Li R, Yang Y, Wu D, Li K, Qin Y, Tao Y and Kong Y 2019 Covalent functionalization of reduced graphene oxide aerogels with polyaniline for high performance supercapacitors† *Chemical Communication* **55** 1738–41
[47] Jurs P C, Bakken G A and McClelland H E 2008 Computational methods for the analysis of chemical sensor array data from volatile analytes *Chem. Rev.* **100** 2649–78
[48] Kim E G, Lee S, Kim J H, Kim C, Byun Y T, Kim H S and Lee T 2012 Pattern recognition for selective odor detection with gas sensor arrays *Sensors* **12** 16262–73
[49] Wu B, Zhao C, Kang J and Wang D 2017 Characteristic study on volatile organic compounds optical fiber sensor with zeolite thin film-coated spherical end *Opt. Fiber Technol.* **34** 91–7
[50] González-Sierra N E, Gómez-Pavón L D C, Pérez-Sánchez G F, Luis-Ramos A, Zaca-Morán P, Muñoz-Pacheco J M and Chávez-Ramírez F 2017 Tapered optical fiber functionalized with palladium nanoparticles by drop casting and laser radiation for H_2 and volatile organic compounds sensing purposes *Sensors* **17** 1–12.
[51] Liao M-S and Scheiner S 2001 Electronic structure and bonding in metal phthalocyanines, Metal = Fe, Co, Ni, Cu, Zn, Mg *J. Chem. Phys.* **114** 9780
[52] Sinha M and Panda S 2015 Effects of thickness, dopant type and doping levels of flexible nanoscale polyaniline films on responses to gases *Material Research Express* **2** 1–16.
[53] Rana M K, Sinha M and Panda S 2018 Gas sensing behavior of metal-phthalocyanines: effects of electronic structure on sensitivity *Chem. Phys.* **513** 23–34